AGU PUBLICATIONS

Geophysical Research Letters

RESEARCH LETTER
10.1002/2014GL060393

Key Points:
- A new state of the EM over the Anthropocene
- Persistent warming since 1750
- Increasing oligotrophy is coupled with warming trend

Supporting Information:
- Readme
- Figure S1
- Figure S2
- Figure S3
- Table S1
- Table S2

Correspondence to:
A. Shemesh,
Aldo.Shemesh@weizmann.ac.il

Citation:
Sisma-Ventura, G., R. Yam, and A. Shemesh (2014), Recent unprecedented warming and oligotrophy of the eastern Mediterranean Sea within the last millennium, *Geophys. Res. Lett.*, *41*, doi:10.1002/2014GL060393.

Received 4 MAY 2014
Accepted 17 JUN 2014
Accepted article online 21 JUN 2014

Recent unprecedented warming and oligotrophy of the eastern Mediterranean Sea within the last millennium

Guy Sisma-Ventura[1], Ruth Yam[1], and Aldo Shemesh[1]

[1]Department of Earth and Planetary Sciences, Weizmann Institute of Science, Rehovot, Israel

Abstract The Mediterranean region is a climatic transitional zone between the subtropical/monsoon regime and the temperate westerlies and is subject to forces acting upon the global climate system. Much knowledge about its climate over the last millennium is derived from terrestrial records, whereas changes in sea surface temperatures (SSTs) and in the dissolved inorganic carbon pool (DIC) are poorly known. We present continuous high-resolution reconstructions of SST and $\delta^{13}C_{DIC}$ in the eastern Mediterranean (EM) Sea, as inferred from oxygen and carbon isotope records from the skeletons of the reef builder gastropod *Dendropoma* sp. Spanning the past millennium, the SST reconstruction reveals a 250 year persistent warming trend during which the twentieth century was the warmest on record. Coupled with a distinct trend of $^{13}C_{DIC}$ depletion and superimposed upon decreased primary production, this climate reconstruction reflects a new state of the EM over the Anthropocene era that exceeds the natural variability of the last millennium.

1. Introduction

The eastern Mediterranean region is a key region for tropical-extratropical interactions [*Fontaine et al.*, 2010]. Sea surface temperatures and deep water formation in the eastern Mediterranean (EM) basin have an important role in preconditioning North Atlantic thermohaline circulation [*Bethoux et al.*, 1999]. In summer, it lies under the dominant influence of the subtropical desert belt, an area where the net fluxes of heat and moisture to the atmosphere result in a warm and salty sea surface layer [*Bethoux et al.*, 1999]. Its thermal variability initiates a global atmospheric teleconnection that influences meridional overturning circulation, deep convection, and precipitation over the Sudan-Sahel region [*Fontaine et al.*, 2010]. The Mediterranean Sea is also considered a sensitive region for climate forcing because of its size and limited exchange with the Atlantic Ocean [*Bethoux et al.*, 1999]. Recently, it has been identified as a climate change "hot spot" in which intensive environmental impacts are expected because of growing anthropogenic pressure [*de Madron et al.*, 2011].

Instrumental observations [*Brunetti et al.*, 2006], documentary data [*Camuffo et al.*, 2010], and terrestrial archives such as lakes, sediments, tree rings, and cave stalagmites [*Jones et al.*, 2006; *Luterbacher et al.*, 2012; *Roberts et al.*, 2012] reveal a complex climatic variability over the last millennium. A limited number of marine records for the last millennium from the Algarian-Balearic Sea (Mg/Ca-based sea surface temperature (SST)) [*Moreno et al.*, 2012] and Ionian Sea (foraminiferal $\delta^{18}O$ and alkenone-based SST) [*Taricco et al.*, 2009; *Versteegh et al.*, 2007] show inconsistent SST trends during the Medieval Warm Period (MWP) and the Little Ice Age (LIA). Low-resolution foraminiferal $\delta^{18}O$ and $\delta^{13}C$ records from the EM Sea show undefined paleo-oceanographic changes during the late Holocene [*Schilman et al.*, 2003, 2001]. Thus, twentieth century trends and anthropogenically induced changes to SST and the dissolved carbonate system must be scaled against preindustrial natural variability derived from high-resolution proxies.

The vermetid *Dendropoma* sp. is a Mediterranean sessile gastropod that forms dense aggregations on rocky shores at the edge of the lower intertidal zone [*Safriel*, 1975], which is part of the shallow EM continental shelf system. The EM shelf lies in close proximity to the deep open water and is characterized by a large annual SST range of 15–30°C, owing to the combined influence of air-sea heat exchange and vertical mixing. Annual salinity variation is relatively small, ranging from 39.0 to 39.6 practical salinity unit (psu). The oxygen and carbon isotopic compositions of vermetid aragonitic skeletons ($\delta^{18}O_{Ver}$ and $\delta^{13}C_{Ver}$) were used to track the cooling of Mediterranean surface water during the LIA [*Silenzi et al.*, 2004; *Sisma-Ventura et al.*, 2009]. However, the exact relationships between the environmental parameters, namely,

mean annual SST, $\delta^{18}O$ of surface seawater ($\delta^{18}O_{sw}$), and $\delta^{13}C$ of dissolved inorganic carbon ($\delta^{13}C_{DIC}$), and their proxies, namely, skeletal $\delta^{18}O_{Ver}$ and $\delta^{13}C_{Ver}$, have yet to be determined.

We conducted 2 years (2009–2010) of sampling of seawater SST, $\delta^{18}O_{sw}$, and $\delta^{13}C_{DIC}$ in four vermetid reef locations in parallel to living vermetid collection for skeletal isotope analyses ($\delta^{18}O_{Ver}$ and $\delta^{13}C_{Ver}$) to establish these relations. We also retrieved five vermetid cores from four locations off the Israeli coast in order to construct a climatic record for the EM over the last millennium.

2. Methods

2.1. General Site Description

The eastern Mediterranean continental shelf is narrow (20 km wide at its southern end and tapering to 10 km wide at its northern end), and therefore, the deep sea is relatively close to the shore. Water circulation over the EM shelf is northward throughout the year with strong seasonal variability. The shelf and slope current system are part of the Levantine basin's general circulation, which is composed of the Atlantic Ionian stream, the Mid-Mediterranean Jet, and the cyclonic basin-wide current that follows the coast [*Gat et al.*, 1996; *Hecht et al.*, 1988]. In summer, the strong currents are confined to the upper layer with seaward intensification. By contrast, in late winter, the slope jet remains offshore and does not intrude over the narrow shelf. During winter storms, strong southwesterly winds drive the northward flowing current and force downwelling over the shelf [*Rosentraub and Brenner*, 2007].

2.2. Seawater Sampling and Analysis

Seawater sampling was designed to establish the relationship between the open shelf water and the water surrounding shore-proximate vermetid reefs during 2009–2010. Surface water from four reef stations along the Israeli coast (Rosh Hanikra (RH), Haazrot Yaasaf (HY), Shiqmona (SQ), and Palmachim (PL; Figure S1 in the supporting information)) was sampled manually and analyzed for isotopic composition ($\delta^{18}O_{sw}$ and $\delta^{13}C_{DIC}$), total alkalinity (A_T), and $^{25°C}pH_{Total}$ on a monthly basis. All stations are not located in the vicinity of large freshwater inputs.

Continental shelf water samples from three stations: Rosh Carmel, Maagan Michael, and Gaash were collected on a seasonal basis, on board the research vessel Mediterranean Explorer.

Total alkalinity and $^{25°C}pH_{NBS}$, measured based on the analytical procedures and calculations described by *Dickson et al.* [2007], were calibrated using certified reference material. The long-term analytical reproducibility of seawater analyses was 0.002 (±1σ standard deviation (SD)) pH units ($n = 333$) and 2 μmol kg^{-1} (±1σ SD; $n = 333$) for alkalinity.

The $\delta^{18}O$ and $\delta^{13}C_{DIC}$ of seawater were analyzed by a Gas Bench II connected in line to a Finnigan MAT 252 mass spectrometer. The results are reported relative to Vienna standard mean ocean water and Vienna Peedee belemnite (VPDB), respectively. The long-term precision of the laboratory working standard is 0.05‰ for $\delta^{18}O$ and 0.08‰ for $\delta^{13}C_{DIC}$.

2.3. Vermetid Sampling and Coring

Living vermetids were collected in the tidal zone from two reef sites (Haazrot Yaasaf and Acziv) for skeletal $\delta^{18}O$ and $\delta^{13}C$ analysis. Each reef top represents an individual abrasion platform [*Safriel*, 1975], with the platforms separated from each other by a few meters to tens of meters. Skeletons from living vermetids (20–40 units) were collected from each reef top and were cleaned by mechanical brushing and sonication and then soaked for several hours in 30% H_2O_2. Powders were homogenized (using mortar and pestle) for each reef top and dried at 50°C for 24 h.

Four sites of shore-proximate reefs along the Israeli coast were drilled: Hof-Dor, Shiqmona, Atlit, and Haazrot Yaasaf (Figure S1). The drilled reefs are composed of a fossil *Denedropoma* and show a thickness of 20–40 cm parallel to the direction of growth. The cores were cut by a diamond headsaw and were cleaned by mechanical brushing and sonication, soaked for several hours in 30% H_2O_2, and dried overnight at 50°C.

Five vermetid cores were used for climate reconstruction. Each core was continuously subsampled at 5 mm intervals using a 1 mm diameter dental drill, which provides a temporal resolution of about 6 years. The

Table 1. Summary of Radiocarbon Measurements

Core ID	Drilling Depth (cm)	Age Year B.P.	Error	Calibrated Year (1σ)	Median	SD	Calibrated Year (2σ)	Median	SD
HD3-10	10	555	30	58–226	142	119	1–234	122	171
HD3-21	21	680	35	148–355	252	146	121–418	270	210
HD3-28	28	790	25	317–429	373	80	284–472	378	133
HD3-33	33	805	30	330–446	388	82	289–483	386	137
HD3-39	39	865	25	410–498	454	62	322–517	420	138
HD3-47	47	1020	25	541–624	583	59	507–655	581	105
SQ2-15	15	565	30	74–234	154	113	40–250	145	148
SQ2-21	21	620	25	138–265	202	90	53–300	177	175
SQ2-31	31	1080	35	553–644	599	64	512–680	596	119
SQ2-37	37	1170	25	634–716	675	58	590–770	680	127
SQ-45	45	1180	25	641–722	682	57	595–785	690	134
AT3-19	19	550	30	50–224	137	123	1–241	121	170
AT3-37	37	725	25	270–380	325	78	230–454	342	138
HD6-35	35	745	25	287–394	341	76	256–450	353	137
HY1-17.5	17.5	1160	25	627–710	669	59	558–756	657	140
HY1-33.5	33.5	1360	25	792–905	849	80	730–947	839	153
SQ4-3	3	1100	25	565–655	610	64	525–690	608	117
SQ4-11.5	11.5	1250	25	678–783	731	74	654–867	761	151
SQ4-22	22	1480	25	921–1029	975	76	875–1113	994	168

subsampling strategy is based on the averaging of 20–40 vermetid units for the same depth layer, which ensures low variability of the isotopic measurements [*Sisma-Ventura et al.*, 2009].

The carbonate powders from vermetid skeletons (200–250 μg) were reacted with 100% H_3PO_4 acid at 25°C and analyzed on a Gas Bench II in line with Finnigan MAT 252. The results are reported relative to the VPDB standard with long-term analytical precision (±1σ SD) of 0.05‰ for $\delta^{13}C$ and 0.08‰ for $\delta^{18}O$. Duplicate reproducibility is 0.05‰ for $\delta^{13}C$ and 0.08‰ for $\delta^{18}O$ ($n = 378$; ±1σ SD).

2.4. ^{14}C Dating

Radiocarbon dating was performed by accelerator mass spectrometry (AMS) in the NOSAMS laboratory (National Ocean Sciences AMS Facility, Woods Hole Oceanographic Institution) on homogenous powders (about 3 mg). Raw radiocarbon dates were converted to calibrated calendar ages by using Calib 6.1 [*Stuiver and Reimer*, 1993] and the additional eastern Mediterranean reservoir age correction of 53 ± 43 ^{14}C year [*Reimer and McCormac*, 2002]. All radiocarbon results are presented in Table 1. An age model was constructed for each core, by fitting a line through 1990 at the core top and through the remaining reservoir-corrected ^{14}C dates. The set intercept was specified for the year 1990, when successful living vermetid populations were still present along the Israeli coast [*Rilov et al.*, 2004]. Individual core records are presented in Figures S2 and S3 in the supporting information.

To construct the composite records, isotopic data from samples of equal age from all five cores were binned, after adjusting overlapping records to a common age. The best-dated cores, HD-3 and SQ-4, were taken as a baseline for minimal peak matching (<20 year) for the remaining cores (AT-3, SQ-2, and HY-1), using AnalySeries [*Paillard et al.*, 1996]. This procedure yielded results that are well within the radiocarbon dating uncertainty (80 year; ±1σ SD). The averaging of data of equal age results in a mean error (±1σ) of 0.07‰ for $\delta^{18}O$ and 0.16‰ for $\delta^{13}C$.

3. Results and Discussion

The 2 year sampling reveals similar average $\delta^{18}O_{sw}$, $\delta^{13}C_{DIC}$, alkalinity, and pH values in reef water (1–2 m deep) and in shelf water (up to 90 m deep) with no clear seasonal variations (Figure 1). Thus, the $\delta^{18}O_{sw}$ and $\delta^{13}C_{DIC}$ values of reef water reflect those of the open water, which suggests that vermetid skeleton deposition occurs under conditions that closely correspond to EM shelf water characteristics. The average $\delta^{18}O_{Ver}$ of living vermetids from reef tops, 0.5‰ ± 0.13‰ (±1σ SD; $n = 300$ individual vermetids), translates to an average deposition temperature [*Bohm et al.*, 2000] of 25.3 ± 0.6°C, taking into account the 2 year average $\delta^{18}O_{sw}$ of 1.6‰. This temperature is approximately 2°C higher than the annual average SST of the EM [*Israel*

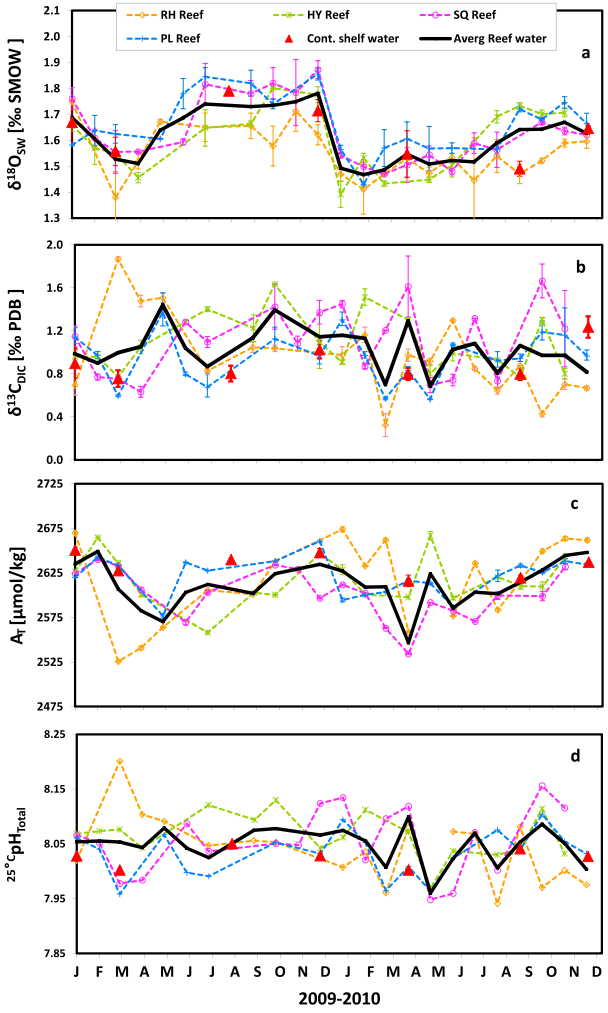

Figure 1. Two years of monthly measurements of the waters surrounding vermetid reefs and the continental shelf water. (a) $\delta^{18}O_{sw}$, (b) $\delta^{13}C_{DIC}$, (c) A_T, and (d) $^{25}{}_{o}C pH_{Total}$ at the four reef stations (RH, HY, SQ, and PL) presented together with the corresponding parameters of continental shelf surface water (red triangles; averaged for the upper 25 m). Vertical error bars denote the duplicate reproducibility (±1σ SD).

Oceanographic and Limnological Research, 2010] due to preferential aragonite deposition during the warm season [*Gentry et al.*, 2008; *Ivany et al.*, 2003]. The average $\delta^{13}C_{Ver}$ of living vermetids, −0.31‰ ± 0.38‰ (±1σ SD; $n = 300$ individual vermetids), is offset by 1.2‰ from the annual average $\delta^{13}C_{DIC}$ of 1.03‰ ± 0.3‰, reflecting the combined isotope effects of calcification and metabolic contribution which range 10–37% in most gastropods [*McConnaughey and Gillikin*, 2008].

The five *Dendropoma* sp. cores show ^{14}C ages spanning from 1480 ± 25 years B.P. to the present, which captures the entire last millennium. The vermetid reef accumulation rates range from 0.5 to 1.04 mm yr^{-1}, with an average of 0.77 ± 0.18 mm yr^{-1} (Table 1). The isotope values of all cores are within the same range with a good agreement in the overlapping periods. The three cores, HD-3, AT-3, and SQ-2, show a pronounce depletion trend in the last 400 years. Cores HY-1 and SQ, which represent the older part of the millennium, show heavier isotopic values. All cores show decadal to centennial fluctuations in both $\delta^{18}O$ and $\delta^{13}C$ records. The continuous composite records, spanning from 975 A.D. to the present, were generated by averaging data from the five cores after adjusting overlapping records to a common age. Overall, the records compare well with the patterns and the isotope values of the previously published results of *Sisma-Ventura et al.* [2009] but presents a better age control, higher resolution, and longer time span. Mean annual SST was reconstructed from the composite $\delta^{18}O_{Ver}$ record by applying the aragonite paleothermometer equation [*Bohm et al.*, 2000]. EM $\delta^{18}O_{sw}$ was assumed to be constant [*Grauel et al.*, 2013] for the SST reconstruction as it is dominated by the advection and mixing of the Atlantic input [*Rohling and Bigg*, 1998], which was stable over the last millennium. The decrease of river discharge, especially due to the Nile damming during the second half of the twentieth century, has resulted with a salinity increase of about 0.3 psu [*Skliris and Lascaratos*, 2004]. Thus, a linear correction of $\delta^{18}O_{sw}$ was applied using the local relationship of $\delta^{18}O_{sw}$/salinity (obtained from all surface data at depth <25 m; $\Delta\delta^{18}O_{sw}/\Delta S = 0.53$) while calculating SST since 1960.

The $\delta^{13}C_{DIC}$ reconstruction was achieved by applying a constant offset of 1.2‰ to the composite $\delta^{13}C_{Ver}$ record (Figure 2).

The EM-SST composite record (Figure 2a) reveals moderate fluctuations, with an amplitude of about 1°C, during the MWP (900–1300 A.D.) [*Moberg et al.*, 2005] and stable SST during the period 1250–1450 A.D. A cooling of about 0.8°C during the LIA (1450–1850 A.D.) [*Moberg et al.*, 2005] began at about 1470 A.D. and culminated at about 1530 A.D. A persistent warming trend started around 1750 and continues until the present. The late 1990s

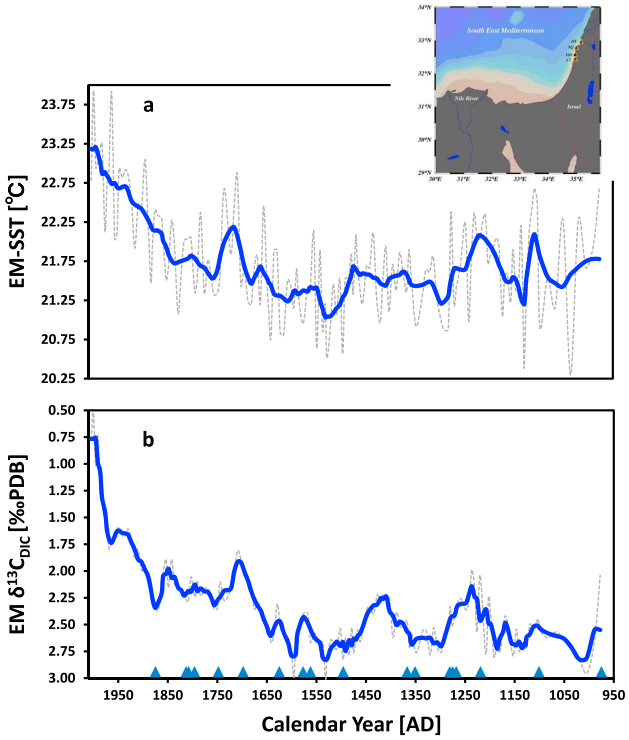

Figure 2. Vermetid-derived sea surface temperature and $\delta^{13}C_{DIC}$ reconstructions for the eastern Mediterranean over the last millennium. (a) EM-SST composite record (dashed gray) and 20 year smoothed trend line (thick blue). (b) EM-$\delta^{13}C_{DIC}$ composite record (dashed gray line) and 20 year smoothed trend line (thick blue). Triangles denote radiocarbon age control. Inset: a map of the study area. The color-coded lines indicate the bathymetry of the EM shelf water.

core top reconstructed SST of 23.2°C agrees well with the EM present mean annual SST of 23.4°C. The EM-SST record is strongly correlated ($r^2 = 0.92$, $n = 42$, $p < 0.001$) with the Italian 250 year instrumental air temperature anomaly [*Brunetti et al.*, 2006] (Figure 3c), with both records showing warming by 2°C since about 1750 A.D. The long-term EM-SST trends are comparable with Northern Hemisphere air temperature reconstructions [*Mann et al.*, 2008; *Moberg et al.*, 2005], with an EM regional amplification factor of 2. This regional amplification was previously identified from 120 year instrumental data [*Metaxas et al.*, 1991]. These correlations suggest that the vermetid-derived SST record mainly reflects Northern Hemisphere changes in air temperatures, amplified for this specific region, and is a reliable proxy for paleo-oceanographic reconstructions.

The different SST and $\delta^{18}O_{sw}$ patterns between the Central and EM records compared to the western Mediterranean records (Figures 3e and 3d), specifically during the Anthropocene since 1750 A.D., also suggests that the recent EM warming trend is not transmitted via the Atlantic input outflow [*Skliris et al.*, 2012] but rather through atmospheric forcing. In general, EM temperatures are linked to the North Atlantic Oscillation (NAO) and the Asian Monsoon [*Jones et al.*, 2006]. A reconstruction of the NAO index over the last millennium shows a persistent positive mode of NAO during the MWP and a negative mode for the LIA [*Trouet et al.*, 2009] (Figure 3f). This feature was identified in marine, lake, and stalagmite records from the western Mediterranean [*Martin-Puertas et al.*, 2010], suggesting NAO forcing of the western Mediterranean climate during the last millennium. However, clear patterns of NAO forcing over the EM are missing from the few marine records from this region [*Roberts et al.*, 2012; *Taricco et al.*, 2009; *Versteegh et al.*, 2007] and lake records from Turkey, Greece, and the Levant [*Roberts et al.,* 2012]. Instead, the strong correlation ($r^2 = 0.76$, $n = 75$, $p < 0.001$) between our EM-SST composite record and the reconstruction of monsoon winds from Arabian Sea sediment cores [*Anderson et al.*, 2002] (Figure 3b) suggests long-term forcing by monsoon circulation over the EM. The positive correlation between the index of the Indian Summer Monsoon and the instrumental SST obtained from the Levantine and Ionian basins was further demonstrated for instrumental records [*Alpert et al.*, 2005; *Raicich et al.*, 2003]. Hence, we attribute the persistent warming trend in the EM since 1750 A.D. to the monsoon-Mediterranean teleconnection, with increases in monsoon circulation increasing the SST of the EM [*Raicich et al.*, 2003].

The reconstructed EM $\delta^{13}C_{DIC}$ record (Figure 4a) shows centennial-scale fluctuations of 0.5–1‰ during the period 975–1750 A.D., followed by a distinct ^{13}C depletion trend of 1.5‰ from 1750 A.D. to the present. The variability between 975 A.D. and 1750 A.D. occurred under stable atmospheric CO_2 concentrations and $\delta^{13}C$ values [*Francey et al.*, 1999]. This suggests that the main influence on $\delta^{13}C_{DIC}$ was primary production rather than SST changes, which were less than 1°C during this period. Primary production in the EM Sea is highly dependent on nutrient delivery by rivers and dust storms [*Herut et al.*, 2002]. Periods of heavy $\delta^{13}C_{DIC}$ are associated with increased productivity because of the preferential uptake of ^{12}C during photosynthesis. At present, the EM is considered to be oligotrophic [*Thingstad et al.*, 2005] because of the limited concentration of phosphate in surface and deep waters. The preindustrial diminishing of the $\delta^{13}C_{DIC}$ cycles since the end of

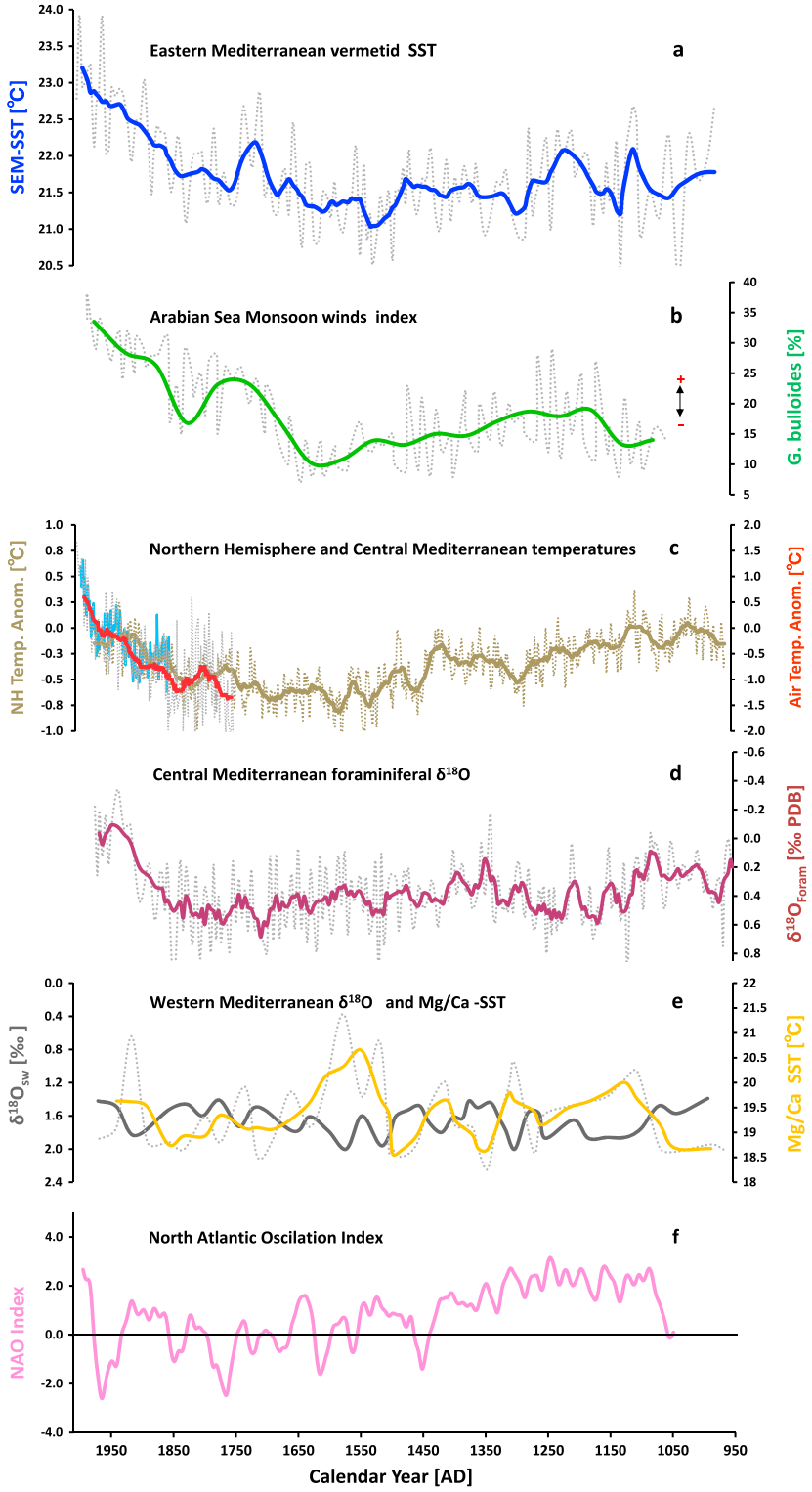

Figure 3. Comparison of EM-SST to Mediterranean and Northern Hemisphere Climate Records. (a) EM-SST composite record (dashed gray line) and 20 year smoothed trend line (thick blue). (b) Monsoon wind strength reconstruction based on foraminifera *G. bulloides* abundance (%) from the Arabian Sea [*Anderson et al.*, 2002] (dashed gray line; 50 year smoothed trend line, thick green). (c) NH air temperature anomaly reconstruction [*Moberg et al.*, 2005] (dashed gray line; 20 year smoothed line, thick brown) presented with the HadCRUT2v (IPCC 2007) instrumental temperature data (blue line, left vertical axis). The Italian 250 year instrumental air temperature anomaly [*Brunetti et al.*, 2006] (red line, right vertical axis). (d) Central Mediterranean, Ionian Sea, South Italy slope foraminiferal $\delta^{18}O$ records [*Taricco et al.*, 2009] (dashed gray line; five-point running average, thick red line). (e) Western Mediterranean, Algarian-Balearic basin, Mg/Ca-based SST (dashed gray line; three-point averaged black line), and $\delta^{18}O_{sw}$ (green line) records [*Moreno et al.*, 2012]. (f) Winter North Atlantic Oscillation (Morocco-Scotland difference; NAO_{ms}) index reconstruction [*Trouet et al.*, 2009] (pink line).

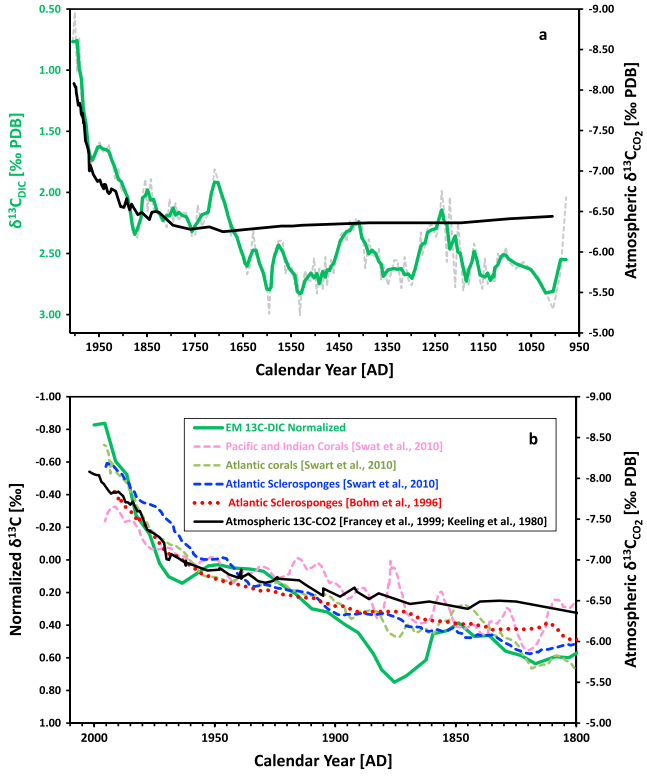

Figure 4. EM $\delta^{13}C_{DIC}$ reconstructions in comparison to atmospheric $\delta^{13}C$-CO_2 and to coral and sclerosponge $\delta^{13}C$. (a) Last millennium composite EM $\delta^{13}C_{DIC}$ (dashed gray line) and 20 year smoothed trend line (thick green) shown with the $\delta^{13}C$ of atmospheric CO_2 from Antarctic ice cores (black line) reconstruction [*Francey et al.*, 1999]. (b) Normalized EM $\delta^{13}C_{DIC}$ (green line) from 1800 to present versus normalized $\delta^{13}C$ records from published data for corals and sclerosponges [*Bohm et al.*, 1996; *Swart et al.*, 2010]. All data were normalized to the mean value $\delta^{13}C$ from 1900 to the present day. Changes in the $\delta^{13}C$ of atmospheric CO_2 (black line) show a similar depletion trend.

the LIA may reflect a transition to a more oligotrophic state. This decreased productivity can be caused by both the warming and drying of the region, probably forced by increased monsoon circulation. Both processes affect nutrient delivery to the surface water by reducing vertical mixing and fresh water input [*Azov*, 1991]. The notable isotopic depletion trend of the industrial era closely follows the records of atmospheric $\delta^{13}C$-CO_2 [*Francey et al.*, 1999] and of the Atlantic and Pacific $\delta^{13}C$ of corals [*Swart et al.*, 2010] and sclerosponges [*Bohm et al.*, 1996] (Figure 4b). This indicates that the Suess effect masks the isotopic signature of productivity in the region. The rate of $\delta^{13}C_{DIC}$ decrease (-0.021‰ yr^{-1}) during the second half of the twentieth century is consistent with the measured rate at which $\delta^{13}C$-CO_2 decreases in the tropical atmosphere [*Keeling et al.*, 2005] (-0.0205‰ yr^{-1} (1977–2008)), and indicates that the EM carbonate system responds rapidly to the anthropogenic addition of CO_2.

The reconstructed SST and $\delta^{13}C_{DIC}$ records show that during the Anthropocene, the EM Sea has reached thermal and primary productivity states that are aberrant for the last millennium. The reconstructed warming rate from 1830 to 2010 of 0.0082°C yr^{-1} is similar to the Mediterranean instrumental warming rate of 0.0086°C yr^{-1} (1904–2006) [*Axaopoulos and Sofianos*, 2009]. At this rate of warming, an increase of about 1°C is expected by the end of the 21st century, during which the mean annual SSTs will be more than 2°C higher than the last millennium's average of 21.6 ± 0.5°C. Thus, with continued global warming, major alternation in thermohaline circulation and deep water formation are expected for the EM Sea. Based on the coupling between temperature and primary production, this process will be accompanied by increasingly oligotrophic conditions, which will have a large impact on the biological ecosystems of the region.

Data supporting Figures 1 and 2 are available as Tables S1 and S2 in the supporting information. Location map, age-depth data, and unspliced $\delta^{18}O$ and $\delta^{13}C$ core records are in Figures S1, S2, and S3, respectively.

Acknowledgments
We thank I. Brailovsky for technical support. This study was funded by the Israel Science Foundation (ISF 742/09).

The Editor thanks Neil Roberts and an anonymous reviewer for their assistance in evaluating this paper.

References

Alpert, P., C. Price, S. O. Krichak, B. Ziv, H. Saaroni, I. Osetinsky, J. Barkan, and P. Kishcha (2005), Tropical tele-connections to the Mediterranean climate and weather, *Adv. Geosci.*, *2*, 157–160.

Anderson, D. M., J. T. Overpeck, and A. K. Gupta (2002), Increase in the Asian southwest monsoon during the past four centuries, *Science*, *297*(5581), 596–599, doi:10.1126/science.1072881.

Axaopoulos, P., and S. Sofianos (2009), Long term variability of sea surface temperature in Mediterranean Sea, paper presented at 7th International Conference of the Balkan-Physical-Union, Alexandroupolis, Greece, 9-13 Sep.

Azov, Y. (1991), Eastern Mediterranean—A marine desert, *Mar. Pollut. Bull.*, *23*, 225–232, doi:10.1016/0025-326x(91)90679-m.

Bethoux, J. P., B. Gentili, P. Morin, E. Nicolas, C. Pierre, and D. Ruiz-Pino (1999), The Mediterranean Sea: A miniature ocean for climatic and environmental studies and a key for the climatic functioning of the North Atlantic, *Prog. Oceanogr.*, *44*(1–3), 131–146, doi:10.1016/s0079-6611(99)00023-3.

Bohm, F., M. M. Joachimski, H. Lehnert, G. Morgenroth, W. Kretschmer, J. Vacelet, and W. C. Dullo (1996), Carbon isotope records from extant Caribbean and south Pacific sponges: Evolution of delta ^{13}C in surface water DIC, *Earth Planet. Sci. Lett.*, *139*(1–2), 291–303, doi:10.1016/0012-821x(96)00006-4.

Bohm, F., M. M. Joachimski, W. C. Dullo, A. Eisenhauer, H. Lehnert, J. Reitner, and G. Worheide (2000), Oxygen isotope fractionation in marine aragonite of coralline sponges, *Geochim. Cosmochim. Acta*, *64*(10), 1695–1703, doi:10.1016/s0016-7037(99)00408-1.

Brunetti, M., M. Maugeri, F. Monti, and T. Nannia (2006), Temperature and precipitation variability in Italy in the last two centuries from homogenised instrumental time series, *Int. J. Climatol.*, *26*(3), 345–381, doi:10.1002/joc.1251.

Camuffo, D., et al. (2010), 500-year temperature reconstruction in the Mediterranean Basin by means of documentary data and instrumental observations, *Clim. Change*, *101*(1–2), 169–199, doi:10.1007/s10584-010-9815-8.

de Madron, X. D., et al. (2011), Marine ecosystems' responses to climatic and anthropogenic forcings in the Mediterranean, *Prog. Oceanogr.*, *91*(2), 97–166, doi:10.1016/j.pocean.2011.02.003.

Dickson, A. G., C. L. Sabine, and J. R. Christian (Eds.) (2007), *Guide to Best Practices for Ocean CO_2 Measurements*, PICES Special Publication 3, 191 pp., North Pacific Marine Science Organization, Sidney, B. C., Canada.

Fontaine, B., J. Garcia-Serrano, P. Roucou, B. Rodriguez-Fonseca, T. Losada, F. Chauvin, S. Gervois, S. Sijikumar, P. Ruti, and S. Janicot (2010), Impacts of warm and cold situations in the Mediterranean basins on the West African monsoon: Observed connection patterns (1979–2006) and climate simulations, *Clim. Dyn.*, *35*(1), 95–114, doi:10.1007/s00382-009-0599-3.

Francey, R. J., C. E. Allison, D. M. Etheridge, C. M. Trudinger, I. G. Enting, M. Leuenberger, R. L. Langenfelds, E. Michel, and L. P. Steele (1999), A 1000-year high precision record of delta ^{13}C in atmospheric CO_2, *Tellus B Chem. Phys. Meteorol.*, *51*(2), 170–193, doi:10.1034/j.1600-0889.1999.t01-1-00005.x.

Gat, J. R., A. Shemesh, E. Tziperman, A. Hecht, D. Georgopoulos, and O. Basturk (1996), The stable isotope composition of waters of the eastern Mediterranean Sea, *J. Geophys. Res.*, *101*(C3), 6441–6451, doi:10.1029/95JC02829.

Gentry, D. K., S. Sosdian, E. L. Grossman, Y. Rosenthal, D. Hicks, and C. H. Lear (2008), Stable isotope and Sr/Ca profiles from the marine gastropod *Conus ermineus*: Testing a multiproxy approach for inferring paleotemperature and paleosalinity, *Palaios*, *23*(3–4), 195–209, doi:10.2110/palo.2006.p06-112r.

Grauel, A. L., A. Leider, M. L. S. Goudeau, I. A. Muller, S. M. Bernasconi, K. U. Hinrichs, G. J. de Lange, K. A. F. Zonneveld, and G. J. M. Versteegh (2013), What do SST proxies really tell us? A high-resolution multiproxy $U^{K'}_{37}$, TEX86H and foraminifera delta O-18) study in the Gulf of Taranto, central Mediterranean Sea, *Quaternary Sci. Rev.*, *73*, 115–131, doi:10.1016/j.quascirev.2013.05.007.

Hecht, A., N. Pinardi, and A. R. Robinson (1988), Currents, water masses, eddies and jets in the Mediterranean Levantine basin, *J. Phys. Oceanogr.*, *18*(10), 1320–1353, doi:10.1175/1520-0485(1988)018<1320:cwmeaj>2.0.co;2.

Herut, B., R. Collier, and M. D. Krom (2002), The role of dust in supplying nitrogen and phosphorus to the Southeast Mediterranean, *Limnol. Oceanogr.*, *47*(3), 870–878.

Israel Oceanographic and Limnological Research (2010), Statistical table for MedGLOSS stations and seasons, MedGLOSS sea level network. [Available at http://medgloss.ocean.org.il/statistic.asp.]

Ivany, L. C., B. H. Wilkinson, and D. S. Jones (2003), Using stable isotopic data to resolve rate and duration of growth throughout ontogeny: An example from the surf clam, *Spisula solidissima*, *Palaios*, *18*(2), 126–137, doi:10.1669/0883-1351(2003)18<126:usidtr>2.0.co;2.

Jones, M. D., C. N. Roberts, M. J. Leng, and M. Turkes (2006), A high-resolution late Holocene lake isotope record from Turkey and links to North Atlantic and monsoon climate, *Geology*, *34*(5), 361–364, doi:10.1130/g22407.1.

Keeling, C. D., S. C. Piper, R. B. Bacastow, M. Wahlen, T. P. Whorf, M. Heimann, and H. A. Meijer (2005), Atmospheric CO_2 and $^{13}CO_2$ exchange with the terrestrial biosphere and oceans from 1978 to 2000: Observations and carbon cycle implications, in *A History of Atmospheric CO_2 and Its Effects on Plants, Animals, and Ecosystems*, edited by J. R. Ehleringer, T. E. Cerling, and M. D. Dearing, p. 83, Springer, New York.

Luterbacher, J., et al. (2012), A review of 2000 years of paleoclimatic evidence in the Mediterranean, in *The Climate of the Mediterranean Region: From the Past to the Future*, edited by P. Lionello, pp. 87–185, Elsevier, Amsterdam, Netherlands.

Mann, M. E., Z. H. Zhang, M. K. Hughes, R. S. Bradley, S. K. Miller, S. Rutherford, and F. B. Ni (2008), Proxy-based reconstructions of hemispheric and global surface temperature variations over the past two millennia, *Proc. Natl. Acad. Sci. U.S.A.*, *105*(36), 13,252–13,257, doi:10.1073/pnas.0805721105.

Martin-Puertas, C., F. Jimenez-Espejo, F. Martinez-Ruiz, V. Nieto-Moreno, M. Rodrigo, M. P. Mata, and B. L. Valero-Garces (2010), Late Holocene climate variability in the southwestern Mediterranean region: An integrated marine and terrestrial geochemical approach, *Clim. Past*, *6*(6), 807–816, doi:10.5194/cp-6-807-2010.

McConnaughey, T. A., and D. P. Gillikin (2008), Carbon isotopes in mollusk shell carbonates, *Geo. Mar. Lett.*, *28*(5–6), 287–299, doi:10.1007/s00367-008-0116-4.

Metaxas, D. A., A. Bartzokas, and A. Vitsas (1991), Temperature-fluctuations in the Mediterranean area during the last 120 years, *Int. J. Climatol.*, *11*(8), 897–908.

Moberg, A., D. M. Sonechkin, K. Holmgren, N. M. Datsenko, and W. Karlen (2005), Highly variable Northern Hemisphere temperatures reconstructed from low- and high-resolution proxy data, *Nature*, *433*(7026), 613–617, doi:10.1038/nature03265.

Moreno, A., et al. (2012), The Medieval Climate Anomaly in the Iberian Peninsula reconstructed from marine and lake records, *Quat. Sci. Rev.*, *43*, 16–32, doi:10.1016/j.quascirev.2012.04.007.

Paillard, D., L. Labeyrie, and P. Yiou (1996), Macintosh Program performs time-series analysis, *Eos. Trans. AGU*, *77*(39), 379–379, doi:10.1029/96EO00259.

Raicich, F., N. Pinardi, and A. Navarra (2003), Teleconnections between Indian monsoon and Sahel rainfall and the Mediterranean, *Int. J. Climatol.*, *23*(2), 173–186, doi:10.1002/joc.862.

Reimer, P. J., and F. G. McCormac (2002), Marine radiocarbon reservoir corrections for the Mediterranean and Aegean Seas, *Radiocarbon*, *44*(1), 159–166.

Rilov, G., Y. Benayahu, and A. Gasith (2004), Prolonged lag in population outbreak of an invasive mussel: A shifting-habitat model, *Biol. Invasions*, *6*(3), 347–364, doi:10.1023/b:binv.0000034614.07427.96.

Roberts, N., et al. (2012), Palaeolimnological evidence for an east-west climate see-saw in the Mediterranean since AD 900, *Global Planet. Change*, *84-85*, 23–34, doi:10.1016/j.gloplacha.2011.11.002.

Rohling, E. J., and G. R. Bigg (1998), Paleosalinity and delta $\delta^{18}O$ A critical assessment, *J. Geophys. Res.*, *103*(C1), 1307–1318, doi:10.1029/97JC01047.

Rosentraub, Z., and S. Brenner (2007), Circulation over the southeastern continental shelf and slope of the Mediterranean Sea: Direct current measurements, winds, and numerical model simulations, *J. Geophys. Res.*, *112*, C11001, doi:10.1029/2006JC003775.

Safriel, U. N. (1975), Role of vermetid gastropods in formation of Mediterranean and Atlantic reefs, *Oecologia*, *20*(1), 85–101, doi:10.1007/bf00364323.

Schilman, B., M. Bar-Matthews, A. Almogi-Labin, and B. Luz (2001), Global climate instability reflected by Eastern Mediterranean marine records during the late Holocene, *Palaeogeogr. Palaeoclimatol. Palaeoecol.*, *176*(1-4), 157–176, doi:10.1016/s0031-0182(01)00336-4.

Schilman, B., A. Almogi-Labin, M. Bar-Matthews, and B. Luz (2003), Late Holocene productivity and hydrographic variability in the eastern Mediterranean inferred from benthic foraminiferal stable isotopes, *Paleoceanography*, *18*(3), 1064, doi:10.1029/2002PA000813.

Silenzi, S., F. Antonioli, and R. Chemello (2004), A new marker for sea surface temperature trend during the last centuries in temperate areas: Vermetid reef, *Global Planet. Change*, *40*(1–2), 105–114, doi:10.1016/s0921-8181(03)00101-2.

Sisma-Ventura, G., B. Guzner, R. Yam, M. Fine, and A. Shemesh (2009), The reef builder gastropod *Dendropoma petraeum*—A proxy of short and long term climatic events in the Eastern Mediterranean, *Geochim. Cosmochim. Acta*, *73*(15), 4376–4383, doi:10.1016/j.gca.2009.04.037.

Skliris, N., and A. Lascaratos (2004), Impacts of the Nile River damming on the thermohaline circulation and water mass characteristics of the Mediterranean Sea, *J. Mar. Syst.*, *52*(1–4), 121–143, doi:10.1016/j.jmarsys.2004.02.005.

Skliris, N., S. Sofianos, A. Gkanasos, A. Mantziafou, V. Vervatis, P. Axaopoulos, and A. Lascaratos (2012), Decadal scale variability of sea surface temperature in the Mediterranean Sea in relation to atmospheric variability, *Ocean Dynam.*, *62*(1), 13–30, doi:10.1007/s10236-011-0493-5.

Stuiver, M., and P. J. Reimer (1993), Extended C-14 data-base and revised CALIB 3.0 C-14 age calibration program, *Radiocarbon*, *35*(1), 215–230.

Swart, P. K., L. Greer, B. E. Rosenheim, C. S. Moses, A. J. Waite, A. Winter, R. E. Dodge, and K. Helmle (2010), The ^{13}C Suess effect in scleractinian corals mirror changes in the anthropogenic CO_2 inventory of the surface oceans, *Geophys. Res. Lett.*, *37*, L05604, doi:10.1029/2009GL041397.

Taricco, C., M. Ghil, S. Alessio, and G. Vivaldo (2009), Two millennia of climate variability in the Central Mediterranean, *Clim Past*, *5*(2), 171–181.

Thingstad, T. F., et al. (2005), Nature of phosphorus limitation in the ultraoligotrophic eastern Mediterranean, *Science*, *309*(5737), 1068–1071, doi:10.1126/science.1112632.

Trouet, V., J. Esper, N. E. Graham, A. Baker, J. D. Scourse, and D. C. Frank (2009), Persistent positive North Atlantic Oscillation mode dominated the Medieval Climate Anomaly, *Science*, *324*(5923), 78–80, doi:10.1126/science.1166349.

Versteegh, G. J. M., J. W. de Leeuw, C. Taricco, and A. Romero (2007), Temperature and productivity influences on $U^{K'}_{37}$ and their possible relation to solar forcing of the Mediterranean winter, *Geochem. Geophys. Geosyst.*, *8*, doi:10.1029/2006GC001543.